Magnetic Resonance in Medicine 53:1143–1149 (2005)

Confidence Mapping in Diffusion Tensor Magnetic Resonance Imaging Tractography Using a Bootstrap Approach

Derek K. Jones[1,2]* and Carlo Pierpaoli[1]

The bootstrap technique is an extremely powerful nonparametric statistical procedure for determining the uncertainty in a given statistic. However, its use in diffusion tensor MRI tractography remains virtually unexplored. This work shows how the bootstrap can be used to assign confidence to results obtained with deterministic tracking algorithms. By invoking the concept of a "tract-propagator," it also underlines the important effect of local fiber architecture or architectural milieu on tracking reproducibility. Finally, the practical advantages and limitations of the technique are discussed. Not only does the bootstrap allow any deterministic tractography algorithm to be used in a probabilistic fashion, but also its model-free inclusion of all sources of variability (including those that cannot be modeled) means that it provides the most realistic approach to probabilistic tractography. Magn Reson Med 53:1143–1149, 2005. Published 2005 Wiley-Liss, Inc.†

Key words: DT-MRI; tractography; deterministic; probabilistic; bootstrap

Diffusion tensor MRI (DT-MRI) fiber tractography is the generic name for a number of algorithms that aim to noninvasively reconstruct the pathways of white matter fasciculi within the brain (1–9). These algorithms can be broadly classified into two types: deterministic and probabilistic. Initial work in the field focused on the former, i.e., deterministic tractography (e.g., 1,2). In this approach, a single pathway is propagated bidirectionally from a "seed point" by moving in a direction that is parallel with the principal eigenvector, ϵ_1, (i.e., the eigenvector associated with the largest eigenvalue). The underlying assumption is that ϵ_1 is parallel to the underlying dominant fiber orientation in each voxel (10). Undoubtedly, this approach can produce anatomically faithful reconstructions of white matter fasciculi (e.g., 11,12) and has proven to be useful in a range of applications (e.g., 13–15).

However, there have been two main criticisms leveled at the deterministic approach. First, deterministic approaches produce only one reconstructed trajectory per seed point, and therefore branching of fasciculi will not, in general, be represented. Second, there is no indication of the confidence that one can assign to a reconstructed trajectory. This is somewhat of a shortcoming as there is uncertainty associated with each estimate of ϵ_1 (16,17) and this uncertainty is nonuniform throughout the brain (17).

Probabilistic tractography algorithms (e.g., 5–7) aim to address both of these criticisms by considering multiple pathways emanating from the seed point and from each point along the reconstructed trajectories. One aim is to allow for the occurrence of branching of fasciculi while another is to quantify the confidence (often referred to as the "probability") that can be assigned to a particular reconstructed pathway. The probability is defined in a number of ways, depending on the algorithm, for example, Koch et al. (7) and Parker et al. (8) have equated the probability of a tract with the number of times it is reconstructed in a Monte Carlo random walk (where the characteristics of the random walk are governed by properties of the diffusion tensor). Tuch et al. (5), on the other hand, assign probability by integrating a cost-function (based on bending energy, etc.) along the path.

Two criticisms that can be leveled at probabilistic algorithms are that (a) either the rules governing the propagation of the reconstructed fasciculi or the formulation of the cost-functions are ad hoc and not rooted in any known anatomic/biologic basis; and (b) the uncertainty is only partly modeled (e.g., 8,9). Although contributions to uncertainty from transient factors, such as "physiologic" noise and system instabilities, are often encountered, a parametric description of these artifacts is generally unavailable. Consequently, these sources of error are not modeled, and so uncertainty is generally modeled based on an assumed Gaussian distribution.

One way to incorporate such random errors in a measure of confidence of the tract reconstruction would be to acquire multiple DT-MRI data sets from a subject and repeat the tracking process from the same anatomic point. However, using each individual data set to generate a single tract from a particular point can prove costly in terms of both scanning time and subject compliance. An alternative approach is to use the bootstrap method (18). This is a nonparametric procedure that enables one to estimate the uncertainty of a given statistic, or its probability density function (PDF), by randomly selecting individual measurements (in this case individual diffusion-weighted images), with replacement, from a set of repeated measurements, thus generating many bootstrap samples. Each bootstrap sample provides a random estimate of a given statistic. Hence, by generating a sufficient number of the bootstrap replicates one obtains a measure of the uncertainty or, in some cases, the PDF of, the given statistic. As

[1]Section on Tissue Biophysics and Biomimetics, Laboratory of Integrative Medicine and Biophysics, National Institute of Child Health and Human Development, National Institutes of Health, Bethesda, Maryland, USA.

[2]Centre for Neuroimaging Sciences, Institute of Psychiatry, London, United Kingdom.

Grant sponsor: Advanced Training Fellowship from the Wellcome Trust to DKJ.

*Correspondence to: Derek K. Jones, Centre for Neuroimaging Sciences, Institute of Psychiatry, P089, De Crespigny Park, London SE5 8AF, United Kingdom. E-mail: d.jones@iop.kcl.ac.uk

Received 3 September 2004; revised 15 December 2004; accepted 22 December 2004 .

DOI 10.1002/mrm.20466
Published online in Wiley InterScience (www.interscience.wiley.com).

the data are drawn with replacement, many more feasible realizations of a DT-MRI volume can be extracted than with a one acquisition = one data set approach.

The bootstrap approach has been used with DT-MRI data to derive PDFs for quantities derived from the diffusion tensor (eigenvalues, trace, anisotropy) (19) and to determine the orientational uncertainty in estimates of the eigenvectors of the tensor (17). Relevant to the current work, Lazar et al. (20) reported the first use of the bootstrap technique in tractography. In this work, we explore this idea in more depth and show how the confidence can be assigned to tractography results obtained using a deterministic algorithm using the bootstrap technique. We also highlight the important effect of the architectural milieu on the reproducibility of tractographic reconstructions. A number of different approaches to visualizing the resulting bootstrap data are investigated.

METHODS

Acquisition

DT-MRI data were acquired from a healthy volunteer on a CNV LX 1.5 GE System with a S3 passive shield magnet and a CRM gradient coil yielding a maximum gradient strength of 50 mT m^{-1} (General Electric, Milwaukee, WI). A standard quadrature birdcage head coil was used for both RF transmission and NMR signal reception. Images were acquired using a multislice single-shot EPI sequence developed in house, optimized for precise measurement of the diffusion tensor in parenchyma (21) and peripherally gated to each cardiac cycle. Whole brain coverage was obtained by collecting 72 contiguous axial slices with isotropic ($2.0 \times 2.0 \times 2.0$ mm) resolution. Four slices were collected per cardiac cycle at trigger delays of 50, 170, 290, and 410 ms after the peripheral pulse trigger (22). The echo time was 90.8 ms and the duration, separation, and strength of the diffusion encoding gradients were 13.4 ms, 42.4 ms, and 49 mT m^{-1}, respectively, giving a maximum diffusion weighting of 1200 s mm^{-2}. The DT-MRI data set consisted of 34 images acquired at each slice location: 4 images acquired with no diffusion gradients applied and 30 diffusion-weighted images in which gradient directions were uniformly distributed in space. This scheme has recently been shown to possess rotationally invariant statistical properties (23). For bootstrap analysis, we collected nine replicates of this DT-MRI data set in a single scanning session, with a total scanning time of 2 hr and 15 min. A vacuum device was used to minimize head motion. Residual subject motion and eddy current induced distortion were corrected using the approach described by Rohde et al. (24). The study protocol was approved by our institutional review board and the subject's consent was obtained prior to scanning.

Bootstrap Analysis

First, all 306 images (i.e., $9 \times (30 + 4)$ images) acquired at each slice location were used to estimate a diffusion tensor in each voxel (10). We refer to this tensor volume as the superset. Subsequently, 4 images acquired with a diffusion weighting close to zero (referred to here as the "$b = 0$ images") and 30 images collected with the trace of the b-matrix equal to 1200 s/mm^2 (i.e., one for each of the 30 unique sampling orientations in the Jones30 scheme) were drawn randomly, with replacement, from the complete set of DWI data. This was performed 5000 times to generate 5000 DT-MRI volumes.

Tractography

A number of seed points were selected, and for both the superset tensor volume and each of the 5000 bootstrapped tensor volumes tractography was performed by launching tracts bidirectionally from the seed point following the direction parallel to the principal eigenvector. The step size was 0.5 mm, and subvoxel stepping was facilitated using the continuous tensor field B-spline approach described by Pajevic et al. (25). Note that, although this approach allows for approximation of the data, we simply interpolated the data as we sought to investigate the inherent variability of the data. The stopping criteria for tracking was an arbitrary threshold of fractional anisotropy (FA) = 0.2. Full details of the tracking algorithm can be found in Basser et al. (4) and Catani et al. (11).

Following Koch et al.'s (7) and Parker et al.'s (8) Monte Carlo approach to tractography, the coordinates of the vertices of the propagated streamlines were binned to the voxel dimensions of the original tensor data. Initially, all voxels in the data set were assigned a value of zero. For each of the 5000 bootstrap iterations, if a voxel was visited by the reconstructed tract, its value was increased by 1. At the end of the 5000th iteration, the number of visits in each voxel was normalized by the total number of bootstraps (i.e., 5000) to generate a "percentage visitation" index. A maximum intensity projection was then obtained (i.e., for each voxel at a particular slice location, the maximum visitation count along the line orthogonal to the plane was computed). These data were then overlaid onto slices showing the fractional anisotropy. In addition to visualizing the visitation data overlaid on anisotropy maps, pathways of individual trajectory reconstructions were using a simple streamline representation. For anatomic reference, these tracts were visualized within a surface rendering of the brain surface, obtained by making an isosurface of the anisotropy data, thresholded at FA = 0.05. All visualizations were performed in MATLAB (The Mathworks, Natick, MA). Note that a preliminary report of this method has appeared previously (26).

RESULTS

Figure 1 shows the results obtained from three seed points placed in the body of the corpus callosum. There is great variability in the reproducibility of the tracking results despite small differences in the location of the seed point and the fact that all three seed points were definitely within the same structure (body of the corpus callosum). Figure 2 shows a result obtained from a seed point placed in the right cerebral peduncle and demonstrates the use of binning the data to give a percentage visitation count. While many of the bootstrapped tracts appear to be inconsistent with known anatomy, the path traced out by the high visitation count appears to give a faithful representation of the fasciculus passing through the cerebral pedun-

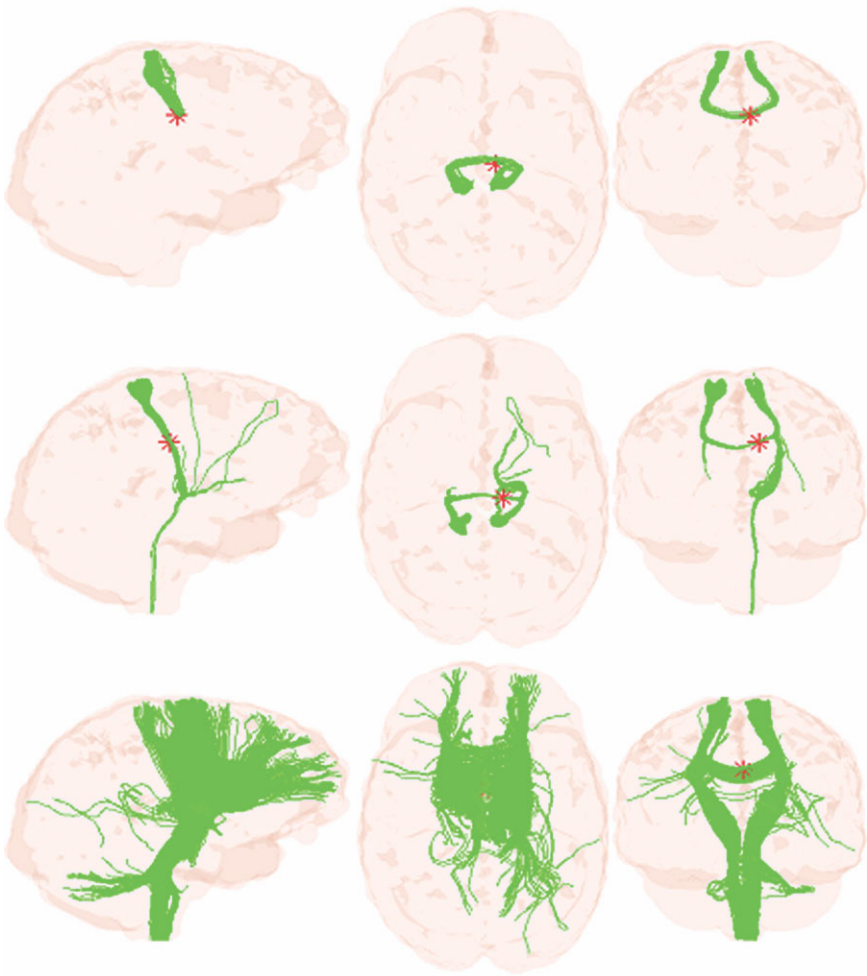

FIG. 1. Bootstrap results obtained from three seed points placed in the body of the corpus callosum. The location of the seed point is indicated by a red asterisk.

cle. The utility of the visitation count maps is further demonstrated in Fig. 3, in which pathways emanating from a point placed in the cingulum are shown. The tract reconstructions are very compact along the central third of the cingulum. This portion of the tract is in local isolation and there are no "alternative " routes/fasciculi in proximity for the stream particle to follow. However, as the streamlines proceed further from the seed point, the tracts begin to deviate and can pick up artifactual false-positive tracts, e.g., connections to the contralateral hemisphere.

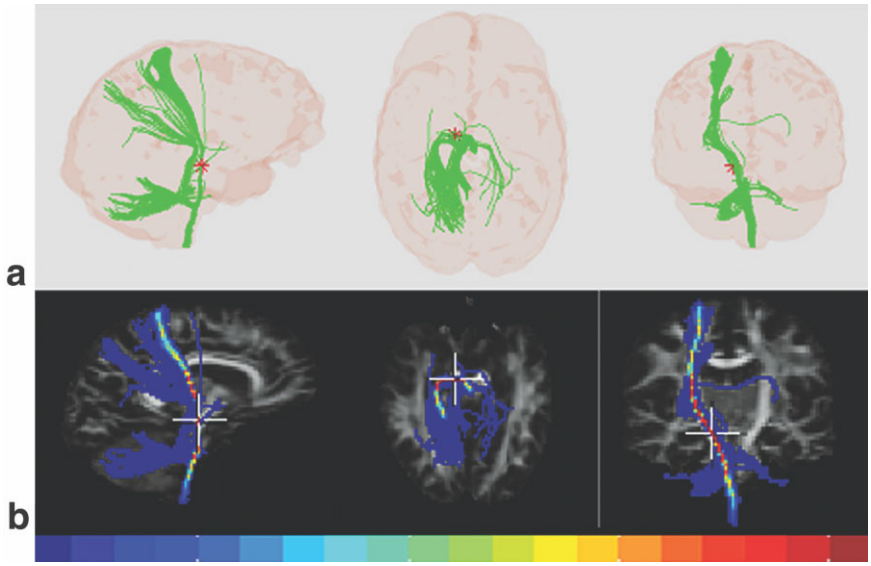

FIG. 2. Results obtained from a seed point placed in the right cerebral peduncle. (a) The "raw" bootstrap trajectories; (b) the percentage visitation count. The color bar is in 5% intervals, with dark blue corresponding to the lowest visitation count (at least 1 visitation), while red corresponds to all 5000 bootstrapped tracts passing through the voxel. The data are overlaid on slices showing the fractional anisotropy (FA). The seed point location is indicated by the cross-hairs.

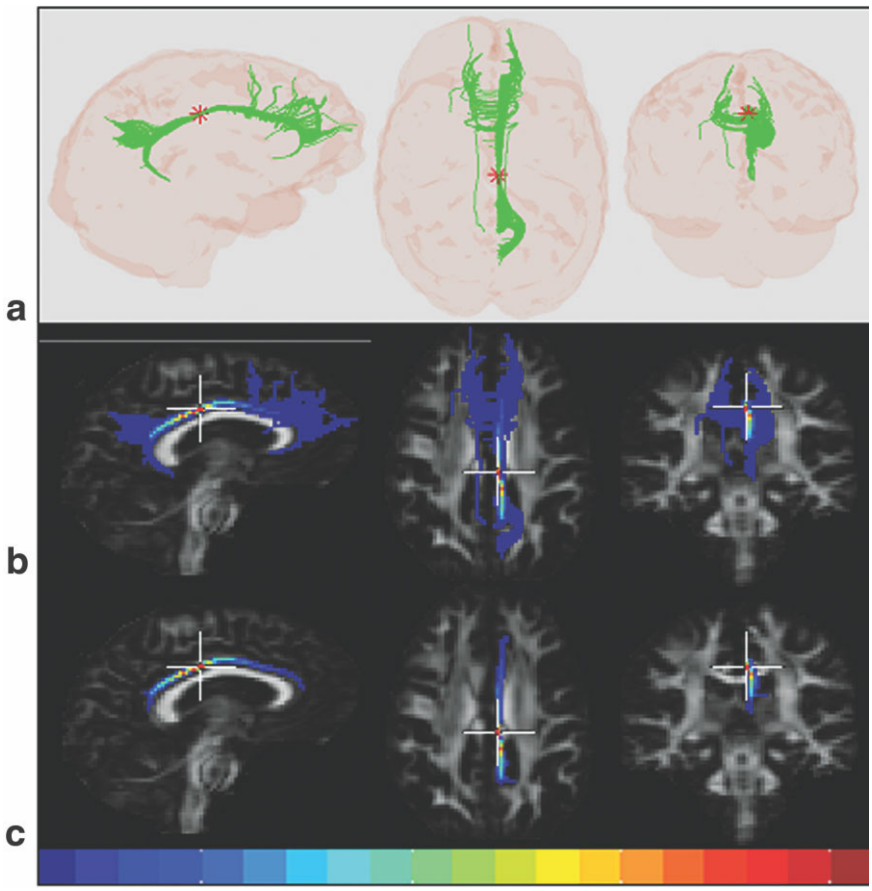

FIG. 3. Results obtained from a seed point placed in the cingulum. (a) The "raw" bootstrap trajectories; (b) the percentage visitation count. The color bar is in 5% intervals, with dark blue corresponding to the lowest visitation count (at least 1 visitation), while red corresponds to all 5000 bootstrapped tracts passing through the voxel. The data are overlaid on slices showing the fractional anisotropy (FA). The seed point location is indicated by the cross-hairs. (c) The same data thresholded at >1% visitation count.

The visitation maps indicate that we should be less confident in these tracts. The 1% threshold (Fig. 2c) results in an anatomically plausible cingulum reconstruction. Finally, Fig. 4 illustrates results obtained from a seed point placed in the left cerebral peduncle. As might be expected, a large portion of the bootstrapped tracts pass along the corticospinal pathway in the ipsilateral hemisphere. However, a considerable portion also cross the pons and ascend the corticospinal pathway in the contralateral hemisphere, which is clearly inconsistent with known anatomy.

DISCUSSION

Bootstrap DT-MRI is a powerful tool for investigating the variability inherent in a number of analyses using DT-MRI data. Bootstrap methods have been previously employed to determine the uncertainty in the principal eigenvector of the diffusion tensor (17), showing a negative relationship between planar anisotropy (27) and the 95% cone of uncertainty of the principal eigenvector. One might therefore predict that tracts launched in a region of high linear anisotropy, and which stay within a region of high linear anisotropy, would be highly reproducible and, likewise, tracts with lower linear anisotropy would be less reproducible. Our results in the anterior portion of the corpus callosum are consistent with this prediction, showing highly reproducible trajectories in a structure with overall high linear anisotropy. However, tracts originating from slightly more posterior seed points in the corpus callosum, although traversing regions with similarly high anisot-

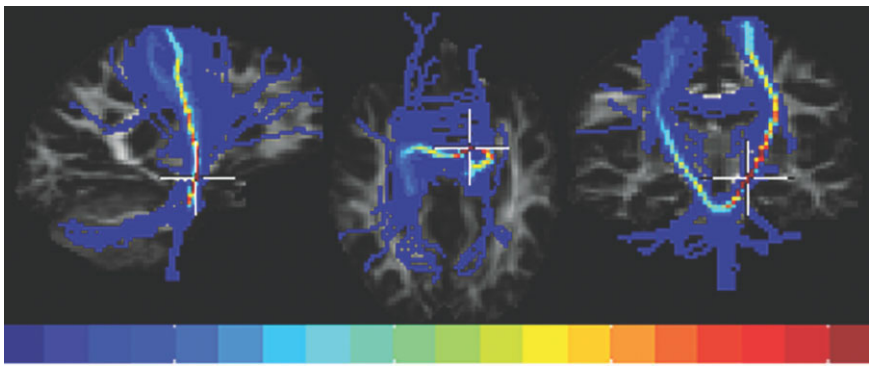

FIG. 4. Visitation map obtained for bootstrapped tracts passing through the left cerebral peduncle (location indicated by cross-hairs). The color scheme is the same as that used in Figs. 2 and 3.

ropy, show a much higher variability of the reconstructed trajectories. Such higher variability could originate from a more marked effect of physiologic noise (e.g., cardiac pulsation) in these regions. Unlike other probabilistic approaches which rely on a priori assumptions about the error distribution, a bootstrap-based tractography approach would be ideally suited to detect such an effect. In our view, however, another important and hitherto unreported factor is the influence of the architectural milieu on the reproducibility of a tract reconstruction. The overall variability in the trajectory of reconstructed tracts is determined not only by the uncertainty in the vector field (which would determine the likelihood of going off track) but also by the characteristics of the surrounding tissue (which would determine what would happen to the off-track trajectories). To better describe this concept, we invoke the notion of a "tract propagator"—i.e., the current position of the "front" of the tract reconstruction. Even in a tract with low and constant uncertainty in its vector field, such as the corpus callosum, the propagator of the reconstructed trajectory could locally progress in a direction inconsistent with the orientation of the anatomic pathway. The consequences of a reconstructed trajectory straying from its true path will be different depending on the type of tissue that the propagator encounters. If the neighboring pathway that the tract propagator picks up is still within the original anatomic structure the effect will be negligible, as the new trajectory will not be anatomically incorrect. Results will also appear reliable if the propagator leaves the structure and encounters either gray matter or CSF. In either case, the anisotropy will generally be lower than the threshold for continuing propagation and so no "false-positive" tracts will be reconstructed. On the other hand, for a tract which passes close to another anatomically distinct pathway a perturbation in the path of the tract propagator can lead to a "leapfrog" of the propagator from one tract to another and a wildly different trajectory is followed, resulting in false-positive reconstructions. We believe that this phenomenon is implicated in explaining the remarkable differences in the reproducibility of tracts launched from different seed points in the corpus callosum. The aberrant trajectories shown in the third panel of Fig. 1 are the consequence of the tract jumping into projection pathways that do not belong to the callosal system anatomically. It is important to note that the "cone of uncertainty" (16,17) in fiber orientation can be small along the entire length of such an erroneous pathway as only a small perturbation is necessary for such a leapfrog to occur.

Note that we have not invoked the term "probability" in relation to this work. There is nothing in the bootstrap approach described here that indicates whether the tract reconstructions are likely to represent real anatomic pathways. Rather, we use the term "confidence mapping" to refer to the amount of confidence we can place in the tract realization not being a spurious "one off" occurrence that has been unusually corrupted by noise, motion, or other sporadic artifacts. A high visitation count (in the binned tract reconstructions) does not mean a high probability of anatomic connection. For example, using a deterministic fiber tractography algorithm to analyze DT-MRI data collected in stroke subjects with a small infarct in the internal capsule, it has been shown that often anatomically incorrect trajectories originate for the corticospinal tract reconstructed on the side of the lesion (28). Specifically, at the level of the pons, the reconstructed pyramidal tract would erroneously cross to the contralateral hemisphere. This was a consequence of the Wallerian degeneration the pyramidal tract fibers, which left the local tensor field dominated by the transverse pontine fibers having left–right orientation. In such a situation, probabilistic tractography approaches, including those based on bootstrapping, would also fail to give a correct indication of the probability of a real anatomic connection. The probabilistic tractography algorithm would detect the high frequency of occurrence of the left–right orientation of the local tensor field, assigning a high probability to the fibers that erroneously cross the pons to the contralateral hemisphere. The result presented in Fig. 4 shows that it is not necessary for such pathology (i.e., Wallerian degeneration) to occur in order for anatomically implausible tractography results to be obtained in this region. In the example shown, the visitation map indicates a reasonably reproducible pathway passing through the left cerebral peduncle, crossing the trans-pontine fibers, and ascending the corticospinal pathway of the contralateral hemisphere—much the same as the result presented by Pierpaoli et al. (28).

Although the anatomic accuracy of DT-MRI tractography needs independent validation, bootstrapping is currently one of the most powerful tools to obtain a reliable assessment of the precision of DT-MRI tractography. Signal variability in diffusion-weighted images is influenced by thermal noise and by spatially and temporally varying artifacts. Such artifacts originate from the so called "physiologic noise," such as subject motion and cardiac pulsation, as well as from acquisition related factors such as system instabilities. While the signal variability produced by thermal noise is approximately Gaussian distributed (29), signal variability produced by physiologic noise and other artifacts does not have a known parametric distribution and currently is impossible to model. It is therefore difficult to include a priori information regarding all variability sources into a probabilistic tractography algorithm and indeed all tractography algorithms proposed to date neglect to include variability originating from artifacts. Bootstrapping tractography is intrinsically sensitive to all sources of variability affecting the DT-MRI data set and bootstrapping results could be used as a benchmark for comparing other probabilistic tractography algorithms. Moreover, bootstrapping can be used to assess the contribution of specific sources of errors to the overall reproducibility of a DT-MRI tractography study. For example, the effect of cardiac gating can be assessed by bootstrapping from supersets containing either gated or ungated data. Furthermore, intrasession, intraday, and long-term reproducibility of tractography results can be assessed by creating bootstrap supersets that include data acquired in a single session (without removing the subject from the magnet), or acquired in the same day, or over several days. Finally, bootstrapping from coregistered data sets from different subjects could provide confidence maps of tractography results for a population.

Given these clear advantages, it would be tempting to suggest that bootstrapping should become the preferred

method for tractography in all clinical and research studies. The main drawback to consider, however, is that the superset must be much larger than the subset whose variability is being characterized. In our study, for example, the superset was nine times larger than the subset. We chose a subset of data that can be collected in a reasonable time for a clinical DT-MRI study, about 15 min. In order to characterize the variability of such a subset, our subject had to lay in the magnet for 2 hr and 15 min, a length of time that is unacceptable for most patients and therefore unsuitable for general clinical use. However, as the SNR of diffusion-weighted acquisitions improves and time efficient acquisition sequences become available, it is not inconceivable that bootstrap analyses could be used in selected groups of cooperative patients in the future. Future work will focus on determining the minimum number of repeat samples taken in each sampling orientation that still permits reliable bootstrap analyses to be performed, with the aim of reducing the time the subject is required to remain in the scanner. We should stress that the results presented here were obtained from a single subject and therefore we are not providing general information regarding the anatomic variability of white matter pathways in healthy human subjects. Indeed, the goal of this paper is not to provide a probabilistic atlas of white matter pathways but rather to describe a new method that allows one to account for the contribution of physiologic noise and other confounds to the variability of fiber trajectories. This approach can be used in a limited number of motivated subjects to compare and contrast the results of probabilistic approaches that require a priori assumptions regarding sources of variability.

Finally, we note that Parker et al. (8) described an algorithm that is similar to the current work, in that a streamlining algorithm is used to infer a measure of probability by incorporating uncertainty in the principal eigenvector. In Parker et al.'s approach, a sigmoidal relationship is assumed between uncertainty in the orientation of the principal eigenvector and the anisotropy and a Monte Carlo random walk is performed, where the orientation of the principal eigenvector is drawn from the distribution defined by the assumed FA/uncertainty relationship. We could have adapted a similar approach, by actually deriving the uncertainties in ϵ_1 in the manner previously described (17), and then use the Monte Carlo approach in the same manner as Parker, the advantage being that the relationship between ϵ_1 uncertainty and anisotropy would be empiric, rather than imposing an assumed model. However, we obviously do not need to rely on the Monte Carlo approach, as we obtain realizations of the distribution of $\epsilon_1$values in "real-time."

CONCLUSIONS

In this work, we have demonstrated the use of the bootstrap technique to generate confidence maps for diffusion tensor tractography results obtained using a deterministic algorithm. We have also highlighted the important influence of the architectural milieu on tractography results. One of the main strengths of the bootstrap approach is that it makes no a priori assumptions regarding the form of the PDF for fiber orientation and thus can account for variability due to non-Gaussian noise (e.g., physiologic noise). The approach reported here can be used to assign confidence to the results obtained with any deterministic tracking algorithm.

REFERENCES

1. Mori S, Crain BJ, Chacko VP, van Zijl PC. Three dimensional tracking of axonal projections in the brain by magnetic resonance imaging. Ann Neurol 1999;45:265–269.
2. Conturo TE, Lori NF, Cull TS, Akbudak E, Snyder AZ, Shimony JS, McKinstry RC, Burton M, Raichle ME. Tracking neuronal fiber pathways in the living human brain. Proc Natl Acad Sci USA 1999;96:10422–10427.
3. Poupon C, Clark CA, Frouin V, Regis J, Bloch I, Le Bihan D, Mangin J. Regularization of diffusion-based direction maps for the tracking of brain white matter fasciculi. NeuroImage 2000;12:184–195.
4. Basser PJ, Pajevic S, Pierpaoli C, Duda J, Aldroubi A. In vivo tractography using DT-MRI data. Magn Reson Med 2000;44:625–632.
5. Tuch DS, Belliveau JW, Wedeen VJ. A path integral approach to white matter tractography. In: Proceedings of the 8th Annual Meeting of ISMRM, Denver, 2000. p. 791.
6. Parker GJM. Tracing fiber tracts using fast marching. In: Proceedings of the 8th Annual Meeting of ISMRM, Denver, 2000. p. 85.
7. Koch M, Glauche V, Finsterbusch J, Nolte U, Frahm J, Buchel C. Estimation of anatomical connectivity from diffusion tensor data. NeuroImage 13:S176, 2001.
8. Parker GJM, Barker GJ, Buckley DL. A probabilistic index of connectivity (PICo) determined using a Monte Carlo approach to streamlines. ISMRM Workshop Diffusion MRI: Biophysical Issues. St Malo, France, March 2002.
9. Behrens TEJ, Johansen-Berg H, Woolrich MW, Smith SM, Wheeler-Kingshott CAM, Boulby PA, Barker GJ, Sillery EL, Sheehan K, Ciccarelli O, Thompson AJ, Brady JM, Matthews PM. Non-invasive mapping of connections between human thalamus and cortex using diffusion imaging. Nat Neurosci 2003;6:750–757.
10. Basser PJ, Mattiello J, Le Bihan D. MR diffusion tensor spectroscopy and imaging. Biophys J 1994;66:259–267.
11. Catani M, Howard R, Pajevic S, Jones DK. Virtual in vivo interactive dissection of white matter fasciculi in the human brain. NeuroImage 2002;17:77–94.
12. Mori S, Kaufmann WE, Davatzikos C, Stieltjes B, Amodei L, Fredericksen K, Pearlson GD, Melhem ER, Solaiyappan M, Raymond GV, Moser HW, van Zijl PCM. Imaging cortical association using diffusion-tensor-based tracts in the human brain axonal tracking. Magn Reson Med 2002;47:215–223.
13. Mori S, Fredericksen K, van Zijl PCM, Stieltjes B, Kraut MA, Solaiyappan M, Pomper MG. Brain white matter anatomy of tumor patients evaluated with diffusion tensor imaging. Ann Neurol 2002;51:377–380.
14. Jones DK, Catani M, Reeves SJ, Shergill SS, McGuire P, Horsfield MA, Simmons A, Williams SCR, Howard RJ. A tractography approach to studying fronto-temporal fasciculi in schizophrenia and late onset schizophrenia-like psychosis. In: Proceedings of the 11th Annual Meeting of ISMRM, Toronto, Canada, 2003. p. 244.
15. Clark CA, Barrick TR, Murphy MM, Bell BA. White matter fiber tracking in patients with space-occupying lesions of the brain: a new technique for neurosurgical planning? NeuroImage 2003;20:1601–1608.
16. Basser PJ. Quantifying errors in fiber tract direction and diffusion tensor field maps resulting from MR noise. In: Proceedings of the 5th Annual Meeting of ISMRM, Vancouver, Canada, 1997. p. 1740.
17. Jones DK. Determining and visualizing uncertainty in estimates of fiber orientation from diffusion tensor MRI. Magn Reson Med 2003;49:7–12.
18. Efron B. Bootstrap methods: another look at the jackknife. Ann Statist 1979;7:1–16.
19. Pajevic S, Basser PJ. Parametric and non-parametric statistical analysis of DT-MRI data. J Magn Reson 2003;161:1–14.
20. Lazar M, Hasan KM, Alexander AL. Bootstrap analysis of DT-MRI tractography techniques: streamlines and tensorlines. In: Proceedings of the 9th Annual Meeting of ISMRM, Glasgow, Scotland, 2001. p. 1527.
21. Jones DK, Horsfield MA, Simmons A. Optimal strategies for measuring diffusion in anisotropic systems by magnetic resonance imaging. Magn Reson Med 1999;42:515–525.

22. Pierpaoli C, Marenco S, Rohde G, Jones DK, Barnett AS. Analyzing the contribution of cardiac pulsation to the variability of quantities derived from the diffusion tensor. In: Proceedings of the 11th Annual Meeting of ISMRM, Toronto, Canada, 2003. p. 70.
23. Jones DK. The effect of gradient sampling schemes on measures derived from diffusion tensor MRI: A Monte Carlo study. Magn Reson Med 2004;51:807–815.
24. Rohde GK, Barnett AS, Basser PJ, Marenco S, Pierpaoli C. Comprehensive approach for correction of motion and distortion in diffusion weighted MRI. Magn Reson Med 2004;51:103–114.
25. Pajevic S, Aldroubi A, Basser PJ. A continuous tensor field approximation of discrete DT-MRI data for extracting microstructural and architectural features of tissue. J Magn Reson 2002;154:85–100.
26. Jones DK, Pierpaoli C. Towards a marriage of deterministic and probabilistic tractography mehtods: bootstrap analysis of fiber trajectories in the human brain. In: Proceedings of the 12th Annual Meeting of ISMRM, Kyoto, Japan, 2004. p. 1276.
27. Westin CF, Peled S, Gudbjartsson H, Kikinis R, Jolesz FA. Geometrical diffusion measures for MRI from tensor basis analysis. In: Proceedings of the 5th Annual Meeting of ISMRM, Vancouver, Canada, 1997. p. 1742.
28. Pierpaoli C, Barnett A, Pajevic S, Chen R, Penix LR, Virta A, Basser P. Water diffusion changes in Wallerian degeneration and their dependence on white matter architecture. NeuroImage 2001;13:1174–1185.
29. Henkelman RM. Measurement of signal intensities in the presence of noise in MR images. Med Phys 1985;12:232–233 (erratum in Med Phys 1986;13:544).